

# Cell Nucleus Image Segmentation Method and Performance Comparison

Shuang Kong, Jie-Sheng Wang\*, Si-Yu Jin

**Abstract**—Image segmentation plays an increasingly important role in clinical medicine and has become an important auxiliary technology for clinical diagnosis of diseases. The shape and size of the nucleus plays a crucial role in treating disease. Therefore, the accurate segmentation of nucleus plays an important role in medical clinical diagnosis. In this paper, SDD segmentation method, adaptive threshold segmentation method, maximum between-class variance method (Otsu) and fuzzy entropy-based segmentation algorithm were used to segment the images of tumor cells and two kinds of human osteosarcoma cells, and the results of accuracy, Dice coefficient and specificity were compared. The results show that the SDD algorithm performs well in accuracy and can segment cell images well. Otsu algorithm has more advantages in eight indexes such as accuracy rate and precision rate. The performance of the adaptive threshold algorithm is not so good as that of the SDD algorithm. The segmentation algorithm based on fuzzy entropy has poor performance and low computational efficiency.

**Index Terms**—Cell image; Partitioning algorithm; Performance index

## I. INTRODUCTION

Image segmentation is the technology and process of extracting the parts needed by the researchers in the image. It is to identify the structure of all the parts needed in the image and mark it out. Image segmentation is an important computer vision technology, including threshold image segmentation, region image segmentation, edge image segmentation and so on[1]. Edge image segmentation is to distinguish edges according to the change rate of gray value, and to segment the image according to the detected edges, which is easy to over-segment the region. Threshold image segmentation using the given threshold to segment the image is simple, but the threshold is difficult to determine; Regional image segmentation is to select a seed point first, and then combine the surrounding points with similar features to

form a subregion. These conventional methods require a lot of human-computer interaction and are easy to be interfered by many factors such as noise[2]. In recent years, convolutional neural networks have achieved good results in image semantic segmentation tasks, and have gradually become a powerful tool for image analysis in various fields of computer vision[3].

Medical image processing is an important field of image segmentation and an important part of computer aided diagnosis system, whose purpose is to segment the required parts of medical images, such as the nucleus, some tissues and organs. Cytopathology is one of the routine methods used by professional physicians in the diagnosis of the disease. By looking at the various types of cell slices produced under the microscope, doctors can diagnose whether a tumor is benign, the degree of differentiation, spread or metastasis of cancer cells, and so on, with the help of cell slices and expertise, because the nucleus contains a large amount of genetic code that controls the cell's shape. Therefore, the detection and segmentation of nucleus is an important task in microscope image analysis. When the number of nuclear samples is large, the cell shapes are different, and the cells overlap, manual segmentation and counting become more difficult. Therefore, when the segmentation technology is applied in the process of nuclear segmentation, the accurate segmentation of the nucleus is a crucial step in the segmentation process, which will affect the performance of the segmentation process[4]. Medical image segmentation is a basic task of intelligent medical diagnosis, aiming at extracting target areas such as organs, tissues or lesions from medical images[5], to provide a more accurate basis for the treatment of diseases. Previously, diseases were diagnosed directly by doctors, and much depended on the knowledge and experience of the doctor. Therefore, since the 1980s, people have actively developed and applied computer-aided diagnosis to improve the detection and diagnostic accuracy of diseases, reduce the workload of doctors, and achieve remote diagnosis[6]. In the last two decades, there have been revolutionary developments in the field of medical image analysis and computer vision, and these advances in the field of medical image processing can be used for segmentation of brain tumors, etc[7]. Deep learning has also experienced exponential growth, with applications in many areas of medicine, especially in the field of medical images, and in medical image segmentation as specific tasks, respectively[8].

On the basis of the gradual maturity of medical information, the application of artificial intelligence technology to disease monitoring, screening, diagnosis and treatment has produced many results and become an

Manuscript received July 31, 2024; revised December 6, 2024. This work was supported by the Basic Scientific Research Project of Institution of Higher Learning of Liaoning Province (Grant No. LJ222410146054), and Postgraduate Education Reform Project of Liaoning Province (Grant No. LNYJG2022137).

Shuang Kong is an undergraduate student of School of Electronic and Information Engineering, University of Science and Technology Liaoning, Anshan, 114051, P. R. China (e-mail: 17742932924@163.com).

Jie-Sheng Wang is a professor of School of Electronic and Information Engineering, University of Science and Technology Liaoning, Anshan, 114051, P. R. China (Corresponding author, phone: 86-0412-2538246; fax: 86-0412-2538244; e-mail: wang\_jiesheng@126.com).

Si-Yu Jin is a postgraduate student of School of Electronic and Information Engineering, University of Science and Technology Liaoning, Anshan, 114051, P. R. China (e-mail: 2468803556@qq.com).

inevitable trend of future development. In the direction of auxiliary diagnosis and treatment of major organ diseases such as liver, intestine, stomach, and breast, computer technology can realize the segmentation of tumors and normal organs, and the judgment of tissue types [9]. Literature [10] used deep learning semantic segmentation for the segmentation of red and white blood cells in blood smear images. The experimental results show that the global accuracy of the model is very high. In literature [11], the segmentation algorithm was used to segment blood cells in microscopic images, and the results showed that the segmentation based on saliency was the most suitable model for the segmentation of white blood cells. In reference [12], an automatic nuclear detection method in cervical cell images was proposed to address such problems as nuclear embedding in folded or overlapping areas of cytoplasm, interference from impurities, low contrast, and changes in the shape and size of nuclei, and experimental results showed that this method performed well. Literature [13] introduced several tumor detection and segmentation methods, including watershed method and bilateral method, due to the variety of segmentation methods for brain tumors. Literature [14] studied medical image segmentation technologies at home and abroad, summarized five medical image segmentation methods based on threshold, edge detection, region growth, fuzzy clustering and deep learning, analyzed their performance, and summarized the research situation of modern medical image segmentation. In this paper, SDD segmentation, adaptive threshold segmentation, Otsu and fuzzy entropy-based segmentation algorithm were used to segment the images of tumor cells and two kinds of human osteosarcoma cells. The structure of the paper is as follows: the second section introduces four image segmentation methods, the third section is experimental simulation and result analysis, and finally the conclusion of the paper.

## II. IMAGE SEGMENTATION METHOD

### A. Otsu

Otsu algorithm is an image segmentation method based on region automatic threshold selection [15]. In the image, it finds an optimal threshold by calculating the variance and inter-class variance of pixels of different gray levels, and divides the image into two regions. The specific steps of the application of this algorithm are as follows:

(1) In the analysis process of segmented image targets, the pixel distribution of each gray level in the image is determined by the number of pixels of each gray level in the segmented image. The probability of this pixel distribution can then be calculated.

(2) In order to measure the effect of image segmentation, it is necessary to calculate the intra-class variance and inter-class variance. The specific operation is: for each possible threshold, the pixels in the image are divided into two parts, one is the pixel whose gray value does not exceed the threshold, and the other is the pixel whose gray value exceeds the threshold. The mean and variance of these two parts of pixels are calculated respectively. The inter-class variance is the difference between the two parts of the pixel variance.

(3) All possible threshold options are needed to determine the optimal segmentation threshold required by this method and calculate the inter-class variance separately. Compare and then find the threshold that maximizes the variance between classes, which is the optimal segmentation threshold.

(4) The optimal segmentation threshold determined in the previous part is used to segment the image, and the image is divided into the foreground part and the background part to realize the binary processing of the image. This step is a key part of the process and can effectively distinguish between different areas of the image.

In the image, Assuming that there are  $m$  gray values, the number of pixels when the gray value is  $i$  is  $n_i$ , then the total number of pixels is obtained:

$$N = \sum_{i=1}^m n_i \quad (1)$$

The probability of the gray value is:

$$P_i = \frac{n_i}{N} \quad (2)$$

Divide them into two groups with the value  $k$  :  $C_0 = [1 \cdots k]$  and  $C_1 = [k+1 \cdots m]$ , then the probability of  $C_0$  group is:

$$\omega_0 = \frac{\sum_{i=1}^k n_i}{N} = \sum_{i=1}^k P_i \quad (3)$$

The probability of group  $C_1$  is:

$$\omega_1 = \frac{\sum_{i=k+1}^m n_i}{N} = \sum_{i=k+1}^m P_i = 1 - \omega_0 \quad (4)$$

The gray value of group  $C_0$  is:

$$u_0 = \frac{\sum_{i=1}^k n_i \times i}{\sum_{i=1}^k n_i} = \frac{\sum_{i=1}^k P_i \times i}{\omega_0} \quad (5)$$

The gray value of group  $C_1$  is:

$$u_1 = \frac{\sum_{i=k+1}^m n_i \times i}{\sum_{i=k+1}^m n_i} = \frac{\sum_{i=k+1}^m P_i \times i}{\omega_1} \quad (6)$$

The overall average gray value is:

$$u = \sum_{i=1}^m P_i \times i \quad (7)$$

When the threshold value is  $k$ , the average value of the gray scale is:

$$u(k) = \sum_{i=1}^m P_i \times i \quad (8)$$

The average gray value of the sample is  $\mu = \omega_0 u_0 + \omega_1 u_1$ , the variance between the two groups is shown in Eq. (9).

$$d(k) = \omega_0 (u_0 - u)^2 + \omega_1 (u_1 - u)^2 \quad (9)$$

So:

$$d(k) = \omega_0 \omega_1 (u_1 - u_2)^2 \quad (10)$$

This changes the value of  $k$  from 1 to  $m$ , obtain  $k^*$ , make  $d(k^*) = \max(d(k))$ . Then, the image is segmented with  $k^*$  as the threshold value, so that the best segmentation effect can be obtained. The advantage of Otsu algorithm is that it does not need to know the distribution of the background and foreground of the image in advance, and it can be automatically applied in different images, so this method is usually applied in the field of image processing.

### B. SDD Segmentation Method

SDD segmentation method [16] is an advanced image processing technology, which can effectively identify significant objects in images. The SDD algorithm performs well in terms of accuracy and can segment cell images well, especially when there are complex structures and subtle differences in the images. The advantage of this method is that the threshold selection method based on slope difference distribution can be flexibly adjusted according to the characteristics of the image, so as to find the optimal threshold for different types of cell or nanoparticle images. Another advantage of this method over the most advanced methods is that because the slope difference distribution contains all thresholds, it can select multiple thresholds at the same time without increasing computational complexity. The procedure for using SDD is as follows:

- (1) Automatic gradient image formation;
- (2) Automatic threshold selection;
- (3) Manually calibrate the threshold selection method for each specific type of cell or nanoparticle image;
- (4) Manually determine the segmentation of each specific type of cell or nanoparticle image;
- (5) After automatically quantifying parameters by iterating morphology erosion, calibrate N and manually determine the segmentation of each specific type of cell or nanoparticle image with one or more typical images.

The SDD segmentation method is more versatile than other state-of-the-art methods in segmenting and quantifying cells or nanoparticles because it takes advantage of a general property of cell and nanoparticle images: intensity and intensity gradients. It enables robust, automatic segmentation and quantification of cells or nanoparticles for a variety of images. The SDD threshold segmentation method can robustly segment different cell or nanoparticle images and their gradient images based on calibration, solving the bottleneck problem and making more general methods universally feasible.

### C. Adaptive Threshold Segmentation Method

Adaptive threshold methods create local thresholds for different image regions. This is called a local or dynamic threshold. Using the threshold method, the pixel value of an object image can be distinguished from the background. The binary threshold sets all pixels with an intensity value above the threshold as foreground values and all remaining pixels as background values to group the image. At the same time, for the traditional threshold operator that uses global thresholds of all pixels, the adaptive threshold will

dynamically change the threshold above the image [17]. According to the brightness distribution of different regions of the image, the local threshold is calculated, so for different regions of the image, different thresholds can be calculated adaptively, so it is called adaptive threshold method.

Let  $f(x, y)$  be the image whose threshold value needs to be obtained, and define its gray scale as  $\{L_0, L_1, L_2, \dots, L_M\}$ , and conduct histogram statistics on the image data, as shown in Eq. (11).

$$P_{L_i} = \frac{n_{L_i}}{N} \quad (11)$$

where,  $n_{L_i}$  represents the gray level of  $L_i$  ( $i=0, 1, \dots, M$ ) the number of pixels,  $N$  is the total number of image pixels.

The images are divided into  $m$  classes by the threshold value  $\delta = \{\delta_1, \delta_2, \dots, \delta_m\}$ , where  $L_0 < \delta_1 < \delta_2 < \dots < \delta_m = L_M$ . For any  $\delta_i \in \delta$ , and  $\delta_1 < \delta_i \leq \delta_m$ , a partition of  $f(x, y)$  can be determined:  $\{\delta_{i-1} + 1, \delta_{i-1} + 2, \dots, \delta_i\}$ , and there is also a partition relative to  $\{P_{L_0}, \dots, P_{L_M}\}$  to  $\{P_{\delta_{i-1}+1}, \dots, P_{\delta_i}\}$ , then the probability of this partition occurring is as follows:

$$P(\delta_i) = \sum_{L_i=\delta_{i-1}+1}^{\delta_i} P_{L_i} \quad (12)$$

Here, the images are divided into three categories, and the segmentation threshold point  $\delta_1, \delta_2, \delta_3$  is set, where  $\delta_3 = L_M$ , the occurrence probabilities of these three categories are:

$$P(\delta_1) = \sum_{L_i=L_0}^{\delta_1} P_{L_i} \quad (13)$$

$$P(\delta_2) = \sum_{L_i=\delta_1+1}^{\delta_2} P_{L_i} \quad (14)$$

$$P(\delta_3) = \sum_{L_i=\delta_2+1}^{L_M} P_{L_i} \quad (15)$$

The overall gray value of the image is:

$$\mu = \sum_{L_i=L_0}^{L_M} L_i P_{L_i} \quad (16)$$

$$\mu(\delta_1) = \sum_{L_i=L_0}^{\delta_1} \frac{L_i P_{L_i}}{P(\delta_1)}, \quad \mu(\delta_2) = \sum_{L_i=\delta_1+1}^{\delta_2} \frac{L_i P_{L_i}}{P(\delta_2)}, \quad \mu(\delta_3) = \sum_{L_i=\delta_2+1}^{L_M} \frac{L_i P_{L_i}}{P(\delta_3)}$$

are the gray average of these three kinds of images.

$$\mu = P(\delta_1)\mu(\delta_1) + P(\delta_2)\mu(\delta_2) + P(\delta_3)\mu(\delta_3) \quad (17)$$

$$\eta(\delta_1) = \sum_{L_i=L_0}^{\delta_1} \frac{L_i P_{L_i}}{P(\delta_1)}, \quad \eta(\delta_2) = \sum_{L_i=\delta_1+1}^{\delta_2} \frac{L_i P_{L_i}}{P(\delta_2)} \quad (18)$$

$$\eta(\delta_3) = \sum_{L_i=\delta_2+1}^{L_M} \frac{L_i P_{L_i}}{P(\delta_3)}$$

$$\mu = \eta(\delta_1) + \eta(\delta_2) + \eta(\delta_3) \quad (19)$$

$$\mu(\delta_1) = \frac{\eta(\delta_1)}{P(\delta_1)}, \quad \mu(\delta_2) = \frac{\eta(\delta_2)}{P(\delta_2)}, \quad \mu(\delta_3) = \frac{\eta(\delta_3)}{P(\delta_3)} \quad (20)$$

Also because:

$$P(\delta_1) + P(\delta_2) + P(\delta_3) = 1 \quad (21)$$

So:

$$\mu(\delta_3) = \frac{\mu - [\eta(\delta_1) + \eta(\delta_2)]}{1 - [P(\delta_1) + P(\delta_2)]} \quad (22)$$

The optimal threshold criterion  $\omega$ , which is the weighted sum of the distance from  $\mu(\delta_1)$ ,  $\mu(\delta_2)$ ,  $\mu(\delta_3)$  to  $\mu$ , is shown in Eq. (23).

$$\omega(L_i) = P(\delta_1)[\mu(\delta_1) - \mu]^2 + P(\delta_2)[\mu(\delta_2) - \mu]^2 + P(\delta_3)[\mu(\delta_3) - \mu]^2 \quad (23)$$

So:

$$(\delta_1, \delta_2) = \arg \max_{L_i \in \{L_0, L_1, \dots, L_M\}} \{\omega(L_i)\} \quad (24)$$

A threshold value  $\delta_1$  is set. When the background radiation is strong, part of the segmentation target is fused with the background. At this time, the threshold value  $\delta_2$  can solve this problem, that is, remove the strong background and obtain the segmentation target.

$$P(\delta_1) = \sum_{L_i=L_0}^{\delta_1} P_{L_i} \quad P(\delta_2) = \sum_{L_i=\delta_1+1}^{\delta_2} P_{L_i} \quad (25)$$

$$\eta(\delta_1) = \sum_{L_i=L_0}^{\delta_1} L_i P_{L_i} \quad \eta(\delta_2) = \sum_{L_i=\delta_1+1}^{\delta_2} L_i P_{L_i} \quad (26)$$

$$\eta(\delta_1) + \eta(\delta_2) = \mu \quad (27)$$

$$P(\delta_1) + P(\delta_2) = 1 \quad (28)$$

So:

$$\omega(L_i) = \frac{[\eta(\delta_1) - \mu P(\delta_1)]^2}{P(\delta_1)[1 - P(\delta_1)]} \quad (29)$$

$$\delta_1 = \arg \max_{\delta_1 \in \{L_0, L_1, \dots, L_M\}} \omega \quad (30)$$

Then  $\delta_1$  is the best threshold of the adaptive threshold algorithm.

#### D. Segmentation method based on fuzzy entropy

The segmentation algorithm based on fuzzy entropy is a technology that uses classified pixels to segment images [18]. This algorithm defines fuzzy membership function to represent the uncertainty of pixels belonging to different regions in the image, and uses fuzzy entropy to measure the uncertainty, so as to achieve image segmentation.

In physical sense, fuzzy entropy and sample entropy are similar to approximate entropy. Approximate entropy is a nonlinear dynamic parameter that can quantify the regularity and unpredictability of time series fluctuations, while sample entropy is an improved method to measure the complexity of time series based on approximate entropy.

In the segmentation algorithm based on fuzzy entropy, the working principle of the algorithm is as follows: Firstly, the fuzzy membership function needs to be defined, which describes the degree to which each pixel in the image belongs to a certain region. Then, the uncertainty of each pixel can be quantified by calculating the fuzzy entropy of each pixel in the image. The higher the fuzzy entropy, the greater the uncertainty that the pixel belongs to a certain region.

The advantage of this algorithm is that it can well deal with the uncertainty and fuzziness in the image, especially when there is a transition area or overlap between the object and the background of the image, the traditional hard segmentation method may not be able to distinguish effectively, while the fuzzy entropy segmentation algorithm can better deal with these cases. The segmentation algorithm based on fuzzy entropy also has its limitations: it has high computational complexity, especially when processing large-scale image data, which may require more computational resources. By introducing the concepts of fuzzy logic and information theory, the segmentation algorithm based on fuzzy entropy aims to overcome the limitations of traditional segmentation methods in dealing with ambiguity and uncertainty in images. Here are some specific ways to do it:

(1) Use generalized fuzzy entropy. The traditional fuzzy entropy segmentation technology usually uses 0.5 as the default value of fuzzy membership degree to segment images. However, the efficiency and accuracy of this method may be greatly reduced when facing images with uneven illumination conditions. In order to improve the segmentation effect, the concept of generalized fuzzy entropy can be introduced, which can evaluate and select the optimal segmentation result more accurately. Because it allows the fuzzy membership value to vary between 0 and 1, a better segmentation method can be chosen.

(2) Use of weighted fuzzy entropy. This weighted fuzzy entropy method can better segment the objects in the graph, so that researchers can get ideal results in segmentation. In image segmentation, weighted fuzzy entropy is used to improve the segmentation effect.

(3) Automatically determine the window width and threshold range of the search. The researchers propose a new method to automatically determine the window width of the membership function based on the grayscale statistical characteristics of the image. The advantage of this method is that no matter what the specific situation of the gray histogram of the image is, it can achieve efficient image segmentation. This method raises the requirement of image segmentation.

### III. SIMULATION AND RESULT ANALYSIS

#### A. Performance Index

Assuming that there are only two types of classification targets, which are counted as positive examples and negative examples, then:

(1) True positives (TP). The number of correctly classified as positive cases, that is, the number of instances classified as positive cases by the classifier and actually are positive cases;



(2) False positives (FP). The number of false positives that are incorrectly classified as positive, that is, the number of instances that are actually negative but are classified as positive by the classifier;

(3) False negatives (FN). The number of false negatives that are incorrectly classified as negative cases, that is, the number of instances that are actually positive cases but classified as negative cases by the classifier;

(4) True negatives (TN). The number of true negatives that are correctly divided into negative cases, that is, the number of instances that the classifier classifies as negative cases and is actually negative cases;

Then the indicators are:

(1) Accuracy

The number of samples of the predicted pair divided by all the samples is called accuracy, and the formula is as follows:

$$Accuracy = \frac{TP + TN}{TP + TN + FP + FN} \quad (31)$$

(2) Precision

The proportion of the number of correctly detected objects to all the detected objects is the accuracy rate. The larger the accuracy rate, the better. 1 is the ideal state.

$$P = \frac{TP}{TP + FP} \quad (32)$$

(3) Dice

In order to solve the conflict between accuracy and recall rate, this index is introduced.

$$Dice = \frac{2 \times precision \times recall}{precision + recall} \quad (33)$$

(4) F-measure

The harmonic average of accuracy and recall is called the F-measure.

(5) Specificity

The larger the value of Specificity, the greater the probability of a healthy specificity being judged as healthy.

$$Specificity = \frac{TN}{TN + FP} \quad (34)$$

(6) Sensitivity

The greater the value of Sensitivity, the smaller FN.

$$Sensitivity = \frac{TP}{TP + FN} \quad (35)$$

(7) Jaccard

$$Jaccard = \frac{TP}{TP + FN + FP} \quad (36)$$

(8) MCC

In the same way as calculating the correlation coefficient between any two variables, you can calculate the correlation coefficient between two binary variables of the real class and the predicted class.

$$MCC = \frac{TP \times TN - FP \times FN}{\sqrt{(TP + FP)(TP + FN)(TN + FP)(TN + FN)}} \quad (37)$$

### B. Tumor Cell Simulation Results

Test 1: Segmentation simulation of tumor cell image.

Three images of tumor cells with size  $696 \times 520$  were selected to be stored in .tif file format for research, as shown in Fig. 1. The true image of the tumor shown is

shown in Fig. 2. Based on these three images, MATLAB simulation is carried out using adaptive threshold segmentation method, Otsu, SDD segmentation method and fuzzy entropy-based segmentation algorithm, and the results of image segmentation by the following segmentation methods are obtained.

The simulation results of tumor cells (1) in Fig. 1 are shown in Fig. 3. With four methods: adaptive threshold segmentation method (adaptive), Otsu, SDD segmentation method and Fuzzy Entropy-based segmentation algorithm (Fuzzy), the average value of three performance indicators is as shown in Table I, the four decimal places are retained, and the optimal value of each performance indicator is bolded. The simulation results of tumor cells (2) in Fig. 1 are shown in Fig. 4. The simulation results of tumor cells (3) in Fig. 1 are shown in Fig. 5.

From the results of tumor cell image segmentation, the four segmentation algorithms have good segmentation effect, and no cells will be missed in the segmentation image. However, in terms of the performance indicators of the four segmentation methods, SDD algorithm performs well in the aspects of accuracy and other performance indicators, and can segment cell images well.

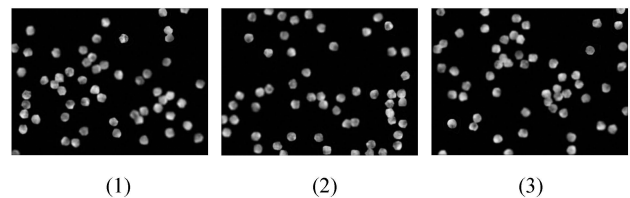


Fig. 1 Tumor cell picture.

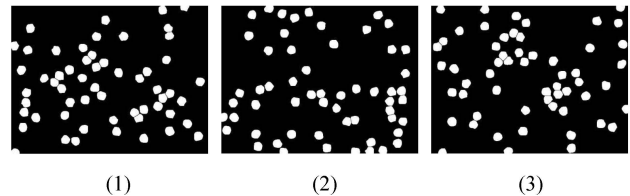


Fig. 2 Tumor cell true picture.

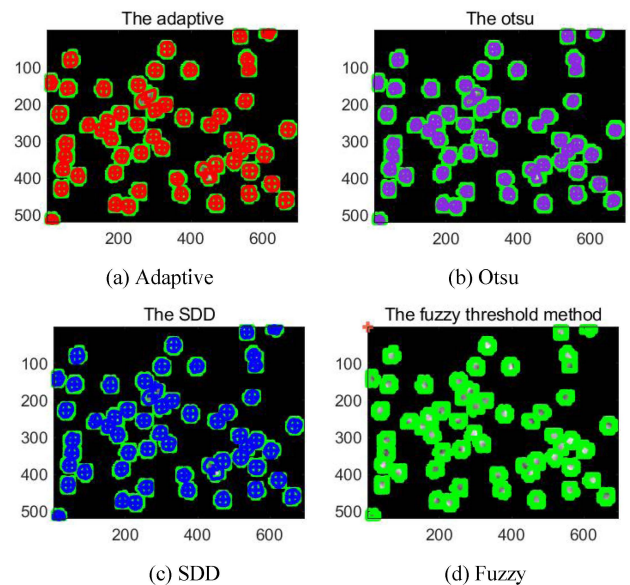


Fig. 3 Simulation results of tumor cell diagram (1).

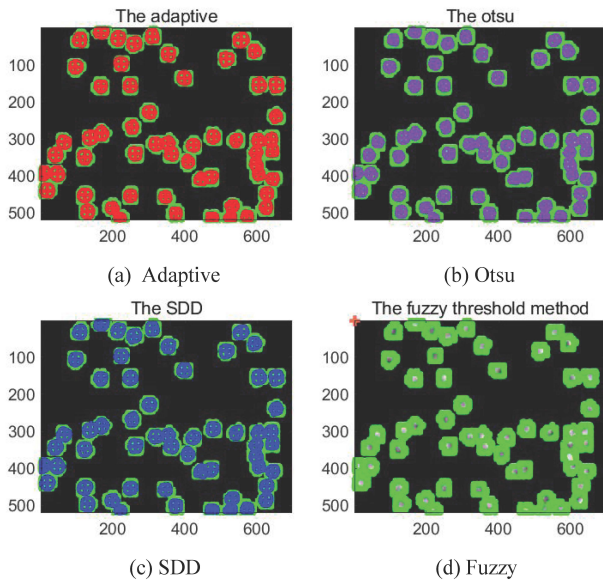


Fig. 4 Simulation results of tumor cell diagram (2).

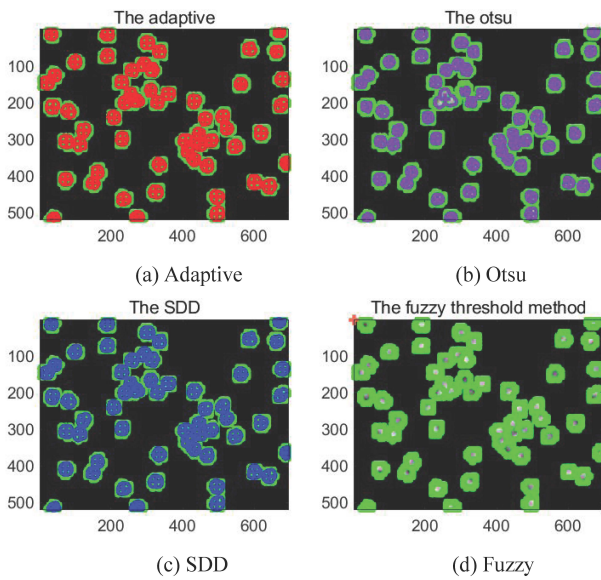


Fig. 5 Simulation results of tumor cell diagram (3).

TABLE I. AVERAGE VALUE OF THREE SIMULATION PERFORMANCE INDICATORS

Performance index	Adaptive	Otsu	SDD	Fuzzy
Accuracy	0.9632	0.9519	<b>0.9643</b>	0.1523
Sensitivity	0.9095	<b>0.9981</b>	0.9149	0.1523
F-measure	0.8748	0.8129	<b>0.8782</b>	0.2644
Precision	0.8426	0.6857	0.8442	<b>1.0000</b>
MCC	0.8542	0.8047	<b>0.8582</b>	NaN
Dice	0.8748	0.8129	<b>0.8782</b>	0.2644
Jaccard	0.7775	0.6848	<b>0.7828</b>	0.1523
Specitivity	0.9721	0.9465	<b>0.9724</b>	NaN

Otsu algorithm has advantages in computational sensitivity, but it is mediocre in other performance indexes. The adaptive threshold algorithm has better performance indicators, but it is slightly inferior to SDD algorithm. The segmentation algorithm based on fuzzy entropy has poor performance in general, but the accuracy is high and the computational efficiency is low.

C. Simulation Results Of The First Human Osteosarcoma Cell

Test 2: The first human osteosarcoma cell image segmentation simulation.

Three images of the first human osteosarcoma cells were selected with size  $1349 \times 1030$  and stored in .tif file format for research, as shown in Fig. 6. The first human osteosarcoma cell diagram is shown in Fig. 7. Based on these three images, MATLAB simulation is carried out using adaptive threshold segmentation method, Otsu, SDD segmentation method and segmentation algorithm based on fuzzy entropy, and the results of image segmentation by the following segmentation methods are obtained.

The simulation results of the first human osteosarcoma cells in Fig. 6(1) are shown in Fig. 8; The simulation results of the first human osteosarcoma cells in Fig. 6(2) are shown in Fig. 9; The simulation results of the first human osteosarcoma cells in Fig. 6(3) are shown in Fig. 10. The first human osteosarcoma cells were divided by four methods and the average value of three performance indicators was shown in Table II (four decimal places were retained). From the image segmentation results, for the first human osteosarcoma cell image, the four segmentation algorithms have good segmentation effect, and there will be no large error.

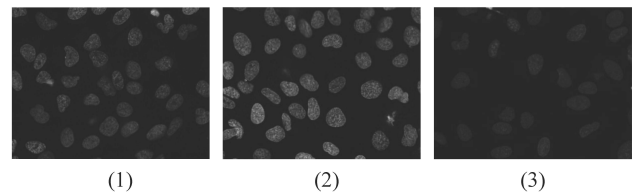


Fig. 6 Picture of the first human osteosarcoma cell.

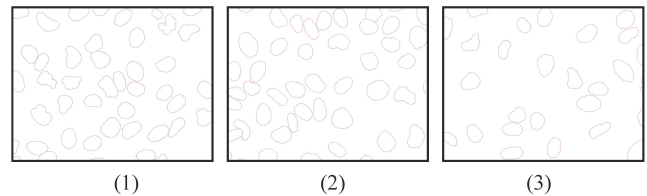


Fig. 7 True picture of the first human osteosarcoma cell.

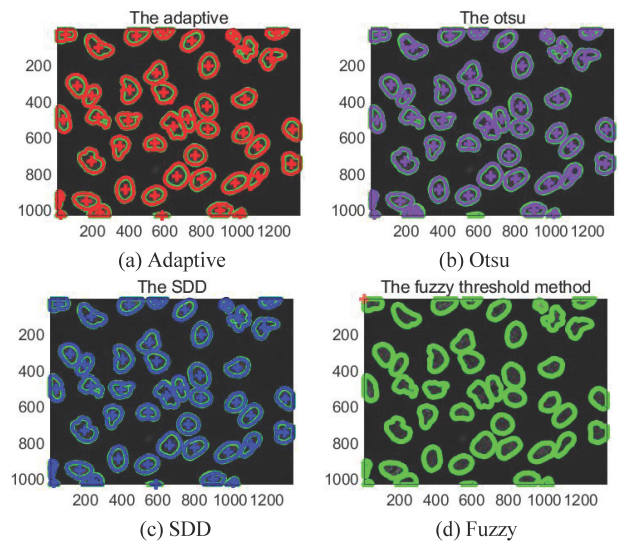


Fig. 8 Simulation results of the first human osteosarcoma cell diagram (1).



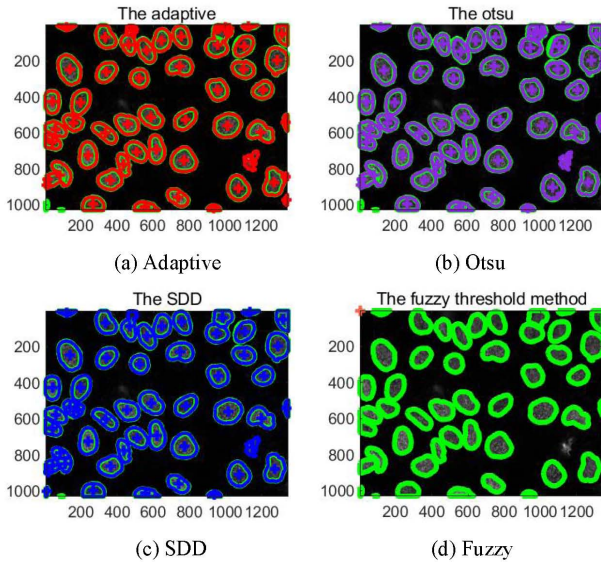


Fig. 9 Simulation results of the first human osteosarcoma cell diagram (2).

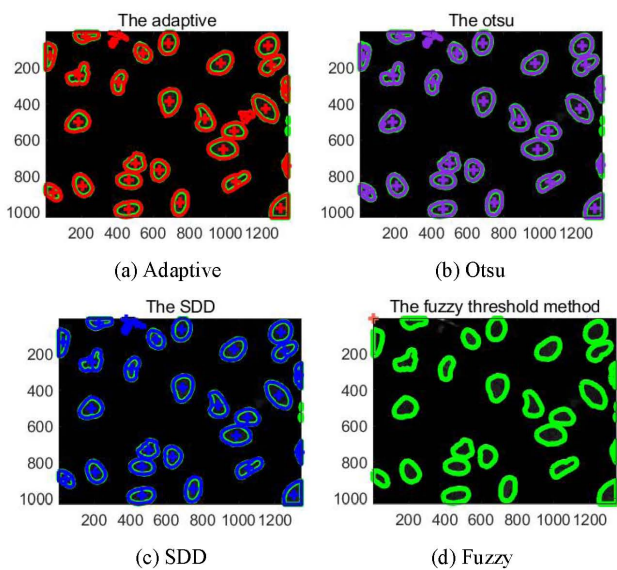


Fig. 10 Simulation results of the first human osteosarcoma cell diagram (3).

TABLE II. AVERAGE VALUE OF THREE SIMULATION PERFORMANCE INDICATORS

Performance index	Adaptive	Otsu	SDD	Fuzzy
Accuracy	0.9652	<b>0.9865</b>	0.9821	0.1542
Sensitivity	0.8639	<b>0.9355</b>	0.8989	0.1542
F-measure	0.9253	<b>0.9572</b>	0.9448	0.2672
Precision	0.9962	0.9798	0.9956	<b>1.0000</b>
MCC	0.9139	<b>0.9495</b>	0.9358	NaN
Dice	0.9253	<b>0.9572</b>	0.9448	0.2672
Jaccard	0.8610	<b>0.9179</b>	0.8953	0.1542
Specitivity	<b>0.9993</b>	0.9963	0.9992	NaN

However, from the performance indicators of the four segmentation methods, Otsu algorithm has excellent performance in accuracy, sensitivity, F-measure, MCC and Jacquard, and can segment cell images better. The adaptive threshold segmentation algorithm has advantages in specific performance indicators, but it is not good in other performance indicators. The SDD algorithm has average performance in computing efficiency and other performance indicators, which is slightly lower than Otsu

algorithm, and better than adaptive threshold segmentation algorithm. The segmentation algorithm based on fuzzy entropy has poor performance in general, low computational efficiency and other performance indicators, but its accuracy is better.

D. Simulation Results Of The Second Human Osteosarcoma Cell

Test 3: Segmentation simulation of the second human osteosarcoma cell image.

Three images of the second kind of human osteosarcoma cells were selected with size  $696 \times 520$  and stored in .tif file format for research, as shown in Fig. 11. The second human osteosarcoma cell diagram is shown in Fig. 12. Based on these three images, four segmentation algorithms are used for MATLAB simulation, and the results of image segmentation by the following segmentation methods are obtained. The simulation results of the second human osteosarcoma cells in Fig. 11(1) are shown in Fig. 13. The simulation results of the second human osteosarcoma cells in Fig. 11(2) are shown in Fig. 14. The simulation results of the second human osteosarcoma cell in Fig. 11(3) are shown in Fig. 15. The average performance indexes of the second human osteosarcoma cells divided three times by four methods are shown in Table III (four decimal places are retained).

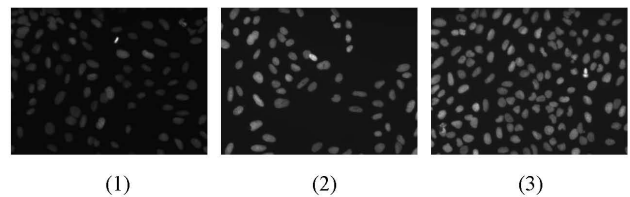


Fig. 11 Picture of the second human osteosarcoma cell.

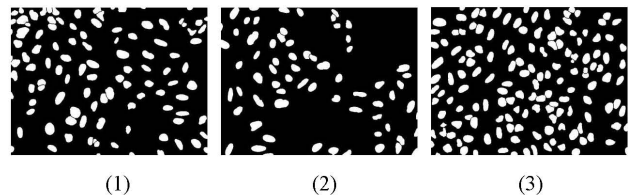


Fig. 12 True picture of the second human osteosarcoma cell.

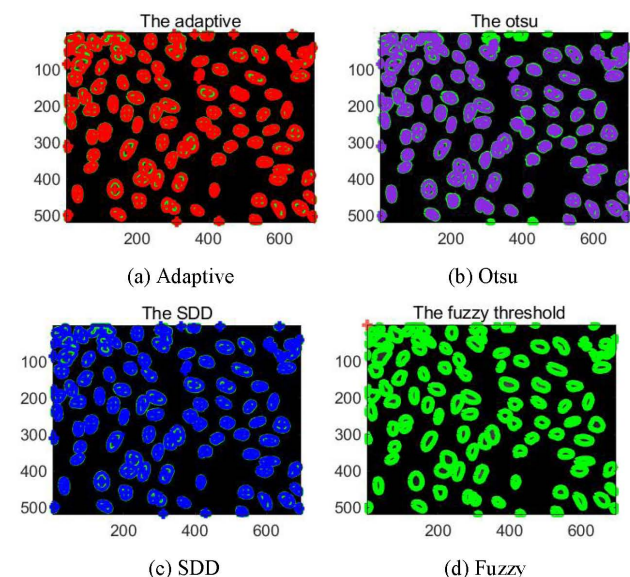


Fig. 13 Simulation results of the second human osteosarcoma cell map (1).



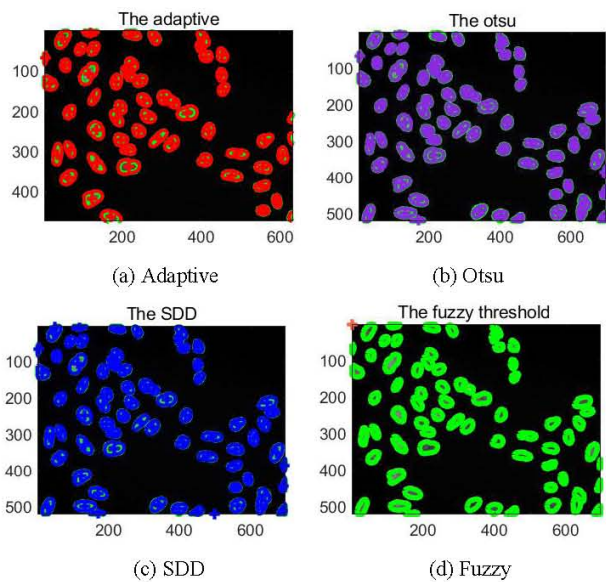


Fig. 14 Simulation results of the second human osteosarcoma cell map (2).

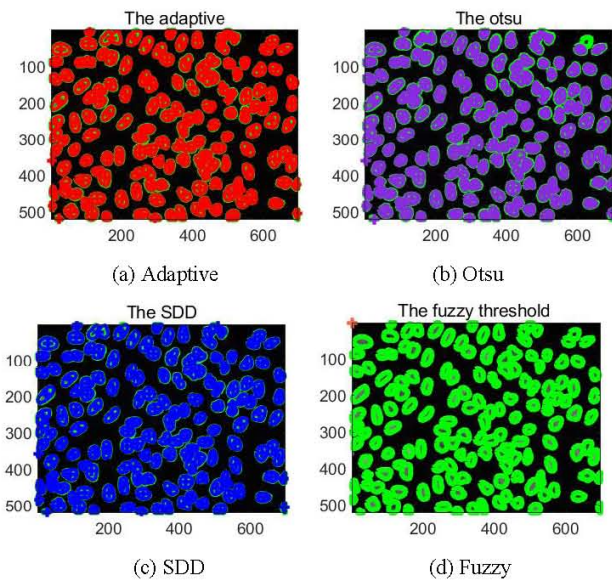


Fig. 15 Simulation results of the second human osteosarcoma cell map (3).

TABLE III. AVERAGE VALUE OF THREE SIMULATION PERFORMANCE INDICATORS

Performance index	Adaptive	Otsu	SDD	Fuzzy
Accuracy	0.9542	<b>0.9697</b>	0.9551	0.2457
Sensitivity	0.8482	<b>0.9315</b>	0.8525	0.2457
Fmeasure	0.9141	<b>0.9387</b>	0.9153	0.3944
Precision	0.9909	0.9460	0.9881	<b>1.0000</b>
MCC	0.8881	<b>0.9186</b>	0.8894	NaN
Dice	0.9141	<b>0.9387</b>	0.9153	0.3944
Jaccard	0.8417	<b>0.8846</b>	0.8438	0.2457
Specitivity	<b>0.9969</b>	0.9823	0.9959	NaN

From the image segmentation results, for the first human osteosarcoma cell image, the four segmentation algorithms have good segmentation effect, and there will be no large error. However, from the performance indicators of the four segmentation methods, the Otsu algorithm has excellent performance in accuracy, sensitivity, F-measure, MCC and

Jacquard, and can segment the second human osteosarcoma cell image better. The adaptive threshold segmentation algorithm has advantages in specific performance indicators, but it is not good in other performance indicators. The performance of SDD algorithm in computing efficiency and other performance indexes is not good, slightly lower than Otsu algorithm, and better than adaptive threshold segmentation algorithm. The segmentation algorithm based on fuzzy entropy has poor performance in general, and the computational efficiency and other performance indexes are low.

#### IV. CONCLUSION

Three kinds of cell images are selected and four kinds of segmentation algorithms are used to achieve different segmentation effects for different cell images. Each of the four image segmentation algorithms has its own advantages and disadvantages. In the actual application of cell image segmentation, the appropriate segmentation algorithm can be selected according to the specific situation and specific needs. If accuracy and precision are the primary factors to consider in image segmentation, you can choose SDD algorithm or Otsu. If there are requirements for performance indicators in terms of comprehensive capability, you can select an adaptive threshold algorithm.

Although image segmentation has been developed for decades, from the practical point of view, image segmentation still needs vigorous research and development. Although each segmentation algorithm has a certain scope of application, on the whole, in the actual operation process, due to the influence of environmental factors, it will have a certain impact on the segmentation results. Therefore, in order to achieve rapid and correct segmentation of clinical medical images, it is necessary to continue research and development and develop more advanced segmentation methods.

#### REFERENCES

- [1] G. Liu, B. Zhou, and W. Xie, "Double Image Segmentation Algorithm for Tick-Mark Recognition of Analog Instrument," *World Journal of Engineering and Technology*, vol. 9, no. 2, pp. 357-373, 2021.
- [2] S. Wang, J. Jiang, and X. Lu. "Advances on Tumor Image Segmentation Based on Artificial Neural Network," *Journal of Biosciences and Medicines*, vol. 8, no. 7, pp. 55-62, 2020.
- [3] X. Jiang, H. Yu, and S. Lv. "An Image Segmentation Algorithm Based on a Local Region Conditional Random Field Model," *International Journal of Communications, Network and System Sciences*, vol. 9, pp. 13, 2020.
- [4] K. Al-Dulaimi, A. Al-Sabaawi, R. D. Resen, and J. J. Stephan, "Using Adapted JSEG Algorithm with Fuzzy C-Mean for Segmentation and Counting of White Blood Cell and Nucleus Images," *Proc. 6th IEEE Asia-Pacific Conf. Comput. Sci. Data Eng. (CSDE 2019)*, IEEE, 2019.
- [5] X. Wang, F. Zhu, Y. Peng, C. Shen, Z. Ye, and C. Zhou, "Semantic Constraint Based Unsupervised Domain Adaptation for Cardiac Segmentation," *Advances in Pure Mathematics*, vol. 11, no. 6, pp. 628-643, 2021.
- [6] E. Matsuyama, "A Novel Method for Automated Lung Region Segmentation in Chest X-Ray Images," *Journal of Biomedical Science and Engineering*, vol. 6, pp. 14, 2021.
- [7] R. M. Sumir, S. Mishra, and N. Shastry, "Segmentation of Brain Tumor from MRI Images using Fast Marching Method," *Proc. IEEE International Conf. Electrical, Computer and Communication Technologies (ICECCT)*, IEEE, 2019.
- [8] A. Luca, T. F. Ursuleanu, L. Gheorghe, R. Grigorovici, S. Iancu, M. Hlusueneac, and C. Preda, "Designing a High-Performance Deep

- Learning Theoretical Model for Biomedical Image Segmentation by Using Key Elements of the Latest U-Net-Based Architectures,” *Electronics*, vol. 11, no. 6, pp. 628-643, 2021.
- [9] J. Wu, T. Yuan, J. Zeng, and F. Gou, “A Medically Assisted Model for Precise Segmentation of Osteosarcoma Nuclei on Pathological Images,” *IEEE Journal of Biomedical and Health Informatics*, vol. 27, no. 8, pp. 3982-3993, 2023.
- [10] T. Tran, O. H. Kwon, K. R. Kwon, S. H. Lee, and K. W. Kang, “Blood Cell Images Segmentation Using Deep Learning Semantic Segmentation,” *Proc. IEEE*, 2018.
- [11] S. M. Sundara, and R. Aarthi, “Segmentation and Evaluation of White Blood Cells using Segmentation Algorithms,” *Proc. 3rd Int. Conf. Trends Electron. Informatics (ICOEI)*, 2019.
- [12] R. Wang, and S. I. Kamata, “Nuclei Segmentation of Cervical Cell Images Based on Intermediate Segment Qualifier,” *Proc. 24th Int. Conf. Pattern Recognit. (ICPR)*, IEEE, pp. 3941-3946, 2018.
- [13] A. E. Babu, A. Subhash, D. Rajan, F. Jacob, and P. A. Kumar, “A Survey on Methods for Brain Tumor Detection,” *Proc. 2018 Conf. Emerg. Devices Smart Syst. (ICEDSS)*, 2018.
- [14] F. Song, Y. Tian, X. Gao, S. Yang, and M. Zheng, “Research on Medical Image Segmentation Method,” *Proc. 3rd Int. Conf. Mach. Learn., Big Data Bus. Intell. (MLBDBI)*, IEEE, pp. 577-580, 2021.
- [15] H. E. Khoukhi, Y. Filali, A. Yahyaouy, M. A. Sabri, and A. Aarab, “A Hardware Implementation of OTSU Thresholding Method for Skin Cancer Image Segmentation,” *Proc. Int. Conf. Wireless Technol., Embedded Intell. Syst. (WITS)*, pp. 1-5, 2019.
- [16] Z. Wang, “A New Approach for Segmentation and Quantification of Cells or Nanoparticles,” *IEEE Transactions on Industrial Informatics*, vol. 12, no. 3, pp. 962-971, 2016.
- [17] L. Atikah, N. A. Hasanah, R. Sarno, A. Fajar, and D. Rahmawati, “Brain Segmentation Using Adaptive Thresholding, K-Means Clustering and Mathematical Morphology in MRI Data,” *Proc. 2019 IEEE Int. Conf. Elect. Comput. Commun. Technol. (ICECCT)*, IEEE, pp. 577-580, 2019.
- [18] I. Y. Maolood, Y. E. A. Al-Salhi, and S. Lu, “Thresholding for Medical Image Segmentation for Cancer using Fuzzy Entropy with Level Set Algorithm,” *Open Medicine*, vol. 14, no. 1, 2018.